Bulletin of the Seismological Society of America, Vol. 93, No. 1, pp. 172–189, February 2003

Empirical Global Depth-Distance Correction Terms for m_b Determination Based on Seismic Moment

by Mehdi Rezapour

Abstract Depth-distance dependent bias in body-wave magnitude is investigated using the International Seismological Centre (ISC) dataset from 1978 to 1993. Large deviations in m_b determination at varying epicentral distances using the Gutenberg and Richter (1956) depth-distance correction terms shows that the correction terms presently used need to be revised. New empirical global depth-distance correction terms $B(\Delta,h)$ for body-wave magnitude are determined using the values of scalar moment M_0 in the Harvard Centroid Moment Tensor (CMT) catalog to calibrate P-wave amplitude-distance curves. Comparison of event magnitude m_b calculated using the Gutenberg–Richter correction terms, and that of this study, shows that the new depth-distance correction terms tend to increase small magnitudes and decrease large magnitudes. Comparison of the correction terms of Gutenberg and Richter, Veith and Clawson (1972), and Lilwall (1987b) with those obtained in this study shows that m_b is biased most when using the correction terms of Gutenberg and Richter (1956). A systematic bias in the estimated m_b for distance greater than 88° is observed for the Veith–Clawson and the Lilwall correction terms. Using Gutenberg–Richter, Veith–Clawson, and Lilwall correction terms, m_b for deep earthquakes is systematically underestimated by about 0.1–0.15, 0.3–0.5, and 0.1–0.2 magnitude units, respectively. Application of the new correction terms to the ISC dataset shows that estimated m_b is then independent of distance and focal depth and hence provides unbiased estimates of m_b in comparison with other correction terms. This observation is also a positive test of the hypothesis that calibration with respect to M_0 gives a better estimate of m_b. Comparison of the standard deviation of m_b values for single events using different depth-distance correction terms shows that the Gutenberg–Richter standard deviations are, on average, larger than those of Veith and Clawson, Lilwall, and this study. Application of station corrections obtained from magnitude residuals reduces the average standard deviations by about 0.07 magnitude unit, which is statistically significant.

Introduction

The body-wave magnitude scale was developed to estimate the size of an earthquake from global short-period (~1 sec) instruments, based on calibration with the surface-wave magnitude scale from long-period (~20 sec) instruments. Gutenberg (1945b) calculated the theoretical ground displacement from a single body wave (*P*, *PP*, and *S*). Then he used the empirical relation of $\log E = 11.3 + 1.8M_s$ (where E is the radiated energy in ergs and M_s is the surface-wave magnitude scale) and corrected the theoretically calculated displacement to the observed displacement of a shallow earthquake. This led to a formulation for body-wave magnitude m_B, based on various seismic phases such as *P*, *PP*, and *S* from shallow-focus earthquakes and calibrated to agree with M_s data available at that time

$$m_B = \log (A/T) + Q(\Delta) + 0.1(m_B - 7) + S_c. \quad (1)$$

Here A is the converted maximum amplitude of body-wave phases on the seismogram to the actual ground-motion amplitude in microns, T is the period of measured signal in seconds, Δ is the epicentral distance in degrees, and S_c is an empirical station correction. $Q(\Delta)$ is the Gutenberg amplitude-distance correction, which was developed by a combination of theory and observation and included effects of both ray geometry and anelastic attenuation (Båth, 1981). In order to reach agreement between m_B and M_s, it was necessary to include in equation (1) a correction term $0.1(m_B - 7)$ for *P*-wave phases, which for very large earthquakes was replaced with $0.2(m_B - 7)$. Gutenberg adjusted m_B to coincide

with his surface-wave magnitude (Gutenberg, 1945a) near M 7.

Gutenberg (1945c) extended his distance correction terms $Q(\Delta)$ by including a depth effect in the calculation of depth-distance correction terms $Q(\Delta,h)$ published in a system of tables and charts. In 1956 Gutenberg and Richter revised the values of $Q(\Delta,h)$ using additional observed data and introduced the unified magnitude m_B as

$$m_B = \log(A/T) + Q(\Delta, h) + S_c. \quad (2)$$

For m_B measurements, various types of seismograph including short- and long-period mechanical instruments and some electromagnetic instruments were used; usually the period of waves used ranges from 0.5 to 12 sec (Kanamori, 1983). Scales obtained from different instruments can be matched at one magnitude level, but they will then diverge at other levels (Scheidegger, 1985). Therefore, any type of magnitude scale gives the size of an earthquake at a particular frequency, so the magnitude is related to the radiation power of seismic waves within a narrow bandwidth, rather than total energy released in the earthquake.

The global agencies such as the International Seismology Centre (ISC) and the National Earthquake Information Center (NEIC) still use equation (2) without station corrections in their determination of body-wave magnitude m_b, but instead of the overall maximum amplitude, a maximum amplitude during the first few cycles of the P-wave on the vertical seismogram of short-period instruments with period $T \leq 3$ sec is used. Therefore, in spite of the essential difference in the period and measurement of amplitude, m_b is now calculated by equation (2), and observations at distances less than 21° or more than 100° are excluded. The main reason for this is to retain temporal catalog homogeneity, at the expense of an inherent bias in m_b, which is the subject of the present study.

Much research has been done in the analysis of P-wave amplitudes, and several amplitude-distance curves containing correction terms for determining body-wave magnitude have been published, for example, Carpenter *et al.* (1967), Cleary (1967), Veith and Clawson (1972), Booth *et al.* (1974), Christoskov *et al.* (1979, 1985, 1991), Vaněk *et al.* (1982), Nortmann and Duda (1982, 1983), Marshall *et al.* (1986), Lilwall (1987a,b), Duda (1989), and Duda *et al.* (1989). The significant differences between published global distance or depth-distance correction schemes, together with the observation of distance and depth bias in m_b estimations, have shown that all the schemes considered contain shortcomings, especially that of Gutenberg and Richter (1956), which is currently used by global agencies such as the ISC and NEIC. The results of many investigations (e.g., Cleary, 1967; Evernden, 1967) suggested that the correction terms of Gutenberg and Richter (1956) could be improved. One possibility is to determine new depth-distance correction terms for m_b using scalar seismic moments from the Harvard Centroid Moment Tensor (CMT) catalog to normalize P-wave amplitude-distance curves.

A more physically based measurement of earthquake size, seismic moment, was introduced into seismology in the middle of last century. Seismic moment rests on the equivalence between elastic dislocation and the double-couple force system (Burridge and Knopoff, 1964; Haskell, 1964). In an earthquake fault, dislocation is equivalent to a distribution of double couples on the fault surface whose total moment is defined by

$$M_0 = \mu A \bar{u}, \quad (3)$$

where μ is the rigidity of the medium and $\bar{u}$ is the average dislocation over a fault plane of area A. Because of the linearity of all the physical laws involved, the excitation of all seismic waves by a point source double couple is proportional to M_0. So the relationship between the logarithm of the seismic moment and magnitude would be expected to be linear. The moment-magnitude relation has the general form

$$\log M_0 = cm + d, \quad (4)$$

where m is the earthquake magnitude and c and d are empirical constants; c depends on the relative time constants of the event and the recording instruments, and d depends on stress drop (Kanamori and Anderson, 1975). However, earthquakes are not point sources, and the distribution of moment release over space and time reduces the observed maximum amplitude for large earthquakes below that for a point source of the same moment. This saturation of the magnitude scale creates nonlinearity between moment and magnitude. Obviously, the moment calculated in equation (4) suffers from all the problems of magnitude determination such as saturation. In particular, since m_b saturates, the estimated value of M_0 using equation (4) for any earthquake with $m_b \gtrsim 6.3$ the estimated M_0 value is probably low. Also, in the case of using surface-wave magnitude, equation (4) fails for very large earthquakes ($M_s \gtrsim 7.3$). Considering the far-field spectrum of a seismic source, we note that the seismic energy of earthquakes concentrates at frequencies below a limit called the corner frequency, which decreases as the size of the earthquake increases. For the large and very large earthquakes, all measurement of the ~1-sec amplitude are taken above the corner frequency. In this study a linear relation is assumed between seismic moment (which correlates to the total radiated energy) and radiated energy by seismic P waves of about 1-sec period (i.e., m_b scale).

Seismologists currently consider the seismic moment to be a more reliable measure of earthquake size, and because of progress in seismological theory and digital instrumentation, moment estimates are made routinely. However, values are available since 1977, and only for a limited number of larger earthquakes. The CMT inversion method utilizes the body-wave data recorded at teleseismic distance. In this

method, the bandpass-filtered waveforms between 22 and 10 mHz (i.e., 45–100 sec) are used (Kawakatsu, 1995). The seismic moment represents the size of an earthquake only at a period much longer than the source process time (≈ source dimension/shear velocity), so it represents the long-period end of the source spectrum (Kanamori, 1983).

Magnitude is not completely related to source physics but it is an empirical measure of source size. We know that because of factors such as radiation pattern, path effects (focusing, defocusing, scattering and attenuation), geology under the station, instrument effect, the assigned magnitudes at different stations will likely come up with different values for the same event. But we don't expect to get different values for magnitude due to the depth-distance correction terms that we use, or to get systematically small or large values at a specific distance for every event no matter what the mechanism and location. The accurate measurement of m_b as a source property is complicated by these effects that are difficult to eliminate without introducing a systematic bias to the scale. Earthquake magnitude, especially m_b, still remains a highly useful term in earthquake hazard analysis; such analysis must usually be derived from archived magnitude data. As the body of global magnitude data increases with the passage of time, there is more scope for understanding, and hence allowing for, its biases and scatter. Bias in m_b values due to any factor directly affects the m_b:M_s criterion for distinguishing explosions from earthquakes, the magnitude-yield relation for explosions, and so forth. In this article, the bias in body-wave magnitude due to inadequate depth-distance correction terms is considered.

The advent of sufficient new source data based on the determination of M_0 since 1978 has given us the opportunity to calibrate the m_b scale with respect to the M_0 scale. Here, new global depth-distance correction terms for body-wave magnitude m_b are developed using widely distributed stations and sources. It is shown that application of the new depth-distance correction terms for the ISC dataset leads to reduction of scatter in station magnitudes, consequently a significant reduction in the standard deviation of event magnitudes (the resulting network-averaged m_b values). By comparing body-wave magnitudes determined using different depth-distance correction terms, it is shown that existing depth-distance correction functions including those of Gutenberg and Richter (1956), Veith and Clawson (1972), and Lilwall (1987b) are depth-distance dependent and that the new function developed in this study represents a statistically significant improvement on its predecessor. Also, the application of station corrections in the determination of m_b is examined.

Data and Method

The ISC dataset from 1978 to 1993, which includes the NEIC catalog, is used in this study. The dataset contains 110,720 events for which the ISC has determined m_b. Of these events, 420 of them have been identified as nuclear explosions, and 75 events have been identified as chemical explosions or events associated with mine blasting, etc. CMT scalar moments are available for a subset of earthquakes having body-wave magnitude ≳5 from 1977. In the CMT catalog the prime location information is that of the NEIC Preliminary Determination of Epicenters (PDE) from its monthly listing. Where NEIC determinations are included in the ISC catalog, they are always from the monthly listing. The NEIC epicentral location and origin time (in the ISC Bulletin) were compared with those in the CMT catalog. Those epicentral estimates whose positions are the same within 0.2 degree in both latitude and longitude and whose times of origin are the same within 5 sec are assumed to be the same earthquake. For the time period 1978 to 1993, 9949 earthquakes with available m_b were matched in this way. Figure 1 shows m_b^{G-R} (m_b that has been determined using the Gutenberg–Richter correction terms) against log M_0 for the these earthquakes. Figure 1a shows the individual data points, and m_b^{G-R} values averaged over 0.1-wide intervals of log M_0 are plotted in Figure 1b with standard deviations. A standard linear regression for these averaged data in the seismic moment range 5.8×10^{16} to 1.0×10^{20} N m gives

$$m_b^{G-R} = (0.389 \pm 0.005) \log M_0 - (1.414 \pm 0.092). \quad (5)$$

Error of parameters in this regression is one standard deviation. By accepting the following assumptions, the *P*-wave amplitude-distance curves from sources with different sizes could be normalized by their different source moments to a unit *P*-wave amplitude-distance curve. (1) The published M_0 values in the CMT catalog have been determined by procedures that did not change systematically during 1978–1993 and give a better estimate of source size than the radiated energy available to Gutenberg (1945b). (2) A linear relation between m_b and logM_0 such as equation (5) as shown in Figure 1b is valid. Here new depth-distance correction terms are obtained for the determination of m_b, using log(A/T) measurements from a large global dataset, normalized to the known M_0 values. In this procedure, tests using different relations between logM_0 and m_b for different depth indicated no improvement overall. Thus, equation (5) is used for all events regardless of depth.

Body-wave magnitude is determined using an empirical relation such as

$$m_b = \log(A/T) + B(\Delta,h), \quad (6)$$

where Δ is epicentral distance in degrees, h is focal depth in kilometers, and $B(\Delta,h)$ is the depth-distance correction term. Substituting equation (6) in (5) gives

$$B(\Delta,h) = 0.389 \log M_0 - 1.414 - \log(A/T). \quad (7)$$

The values of $B(\Delta,h)$ according to equation (7) were calcu-

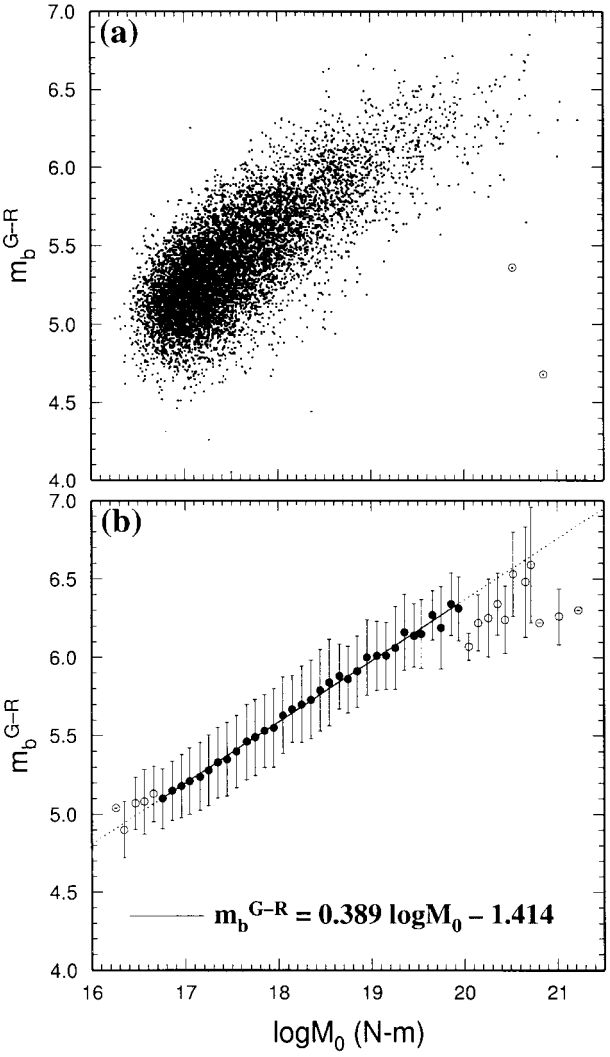

Figure 1. m_b^{G-R} against log M_0 for 9949 earthquakes. (a) Individual data; (b) Averaged m_b^{G-R} values over 0.1-wide intervals of log M_0. The two circled earthquakes in (a) were thought to be in error and were not used in the averaging process. In (b) the solid line represents a linear regression to the data in the seismic moment range 5.8×10^{16} to 1.0×10^{20} N m. The data points in this range are shown by filled circles.

lated for 478,122 amplitude/period measurements in the dataset from the 9949 earthquakes in the depth intervals 0–35, 35–70, 70–150, 150–300, 300–500, and 500–650 km. Table 1 summarizes the data that were selected. The $B(\Delta,h)$ values in each depth interval were averaged over 1-degree-wide distance intervals to produce a depth-distance correction curve at the mean of each depth interval. These curves were then smoothed using the kernelsmoother (Venables and Ripley, 1999) as $\hat{y}_i = \sum_{j=1}^{n} y_i K\left(\frac{x_i - x_j}{b}\right) \Big/ \sum_{j=1}^{n} K\left(\frac{x_i - x_j}{b}\right)$ (where $\hat{y}_i$ is smoothed value at x_i, n is total number of data points, b is a bandwidth parameter, and K is a kernel function which is taken to be a standard normal density) and are plotted in Figure 2. For bandwidth b, the optimum value is 3 degrees. Because of uncertainty in determined zero depth (artificially constrained to zero), the depth-distance correction curve for zero depth was derived by adding 0.05 to depth-distance correction curve at 15 km. Also, due to data lack for $h \geq 650$ km (see Table 1), the deepest correction curve, that is, the depth-distance correction curve at 730 km depth was derived by subtracting 0.15 from depth-distance correction curve at 550 km.

Table 1
Summary of the Data Which Were Used to Obtain Depth-Distance Correction Curves B (Δ,h)

Depth Range (km)	Approximate Mean Depth (km)	Number of Earthquakes	Number of Log (A/T)
$0 \leq h < 35$	15	4997	236748
$35 \leq h < 70$	50	2289	107648
$70 \leq h < 150$	100	1338	64233
$150 \leq h < 300$	200	631	33053
$300 \leq h < 500$	400	229	14130
$500 \leq h < 650$	550	454	21983
$h \geq 650$	—	11	327

The term 0.389 logM_0 in equation (7) normalizes the amplitude-distance curves of the P waves from earthquakes of different sizes. Suppose seismic moments of two events with the same focal depth are 1.0×10^{17} and 1.0×10^{20} N m. From the term 0.389 logM_0 in equation (7) for normalizing P-wave amplitude-distance curves, an offset in magnitude between P-wave amplitude-distance curves for these two events of $1.167 = 3 \times 0.389$ magnitude units is assumed. This proposed offset depends on the coefficient of logM_0 in equation (7) or equation (5). A small value for the coefficient of logM_0 was found to give a slightly smoother $B(\Delta,h)$ curve than a large value. Increasing the coefficient of logM_0 in equation (7) was found to affect the slope of $B(\Delta,h)$; the curves increase at $\Delta > 85°$, and this gave a negative station residual, namely, m_b(event) $< m_b$(station) at distance range of $\Delta > 85°$. The reverse becomes true as the coefficient of logM_0 is decreased. The increase in $B(\Delta,h)$ beyond a range of $\Delta > 85°$ is due to the core shadow transition or *PKP* zone where the P-wave amplitude is quickly reduced with distance, thus in the distance range of $85° < \Delta < 100°$ the observed amplitudes are small and the sources generally large. Large sources lead to potentially large correction if the coefficient of logM_0 is large. By decreasing or increasing the coefficient of logM_0, the $B(\Delta,h)$ curves obtained do not change significantly for the distance range of $21° \leq \Delta \leq 85°$.

As an example the procedure of normalizing P-wave amplitude distance curves was repeated using the ratio of $\frac{\log(A/T)}{\log M_0}$ (i.e., coefficient of logM_0 is one), but in general the $B(\Delta,h)$ curves obtained using equation (7) give better results

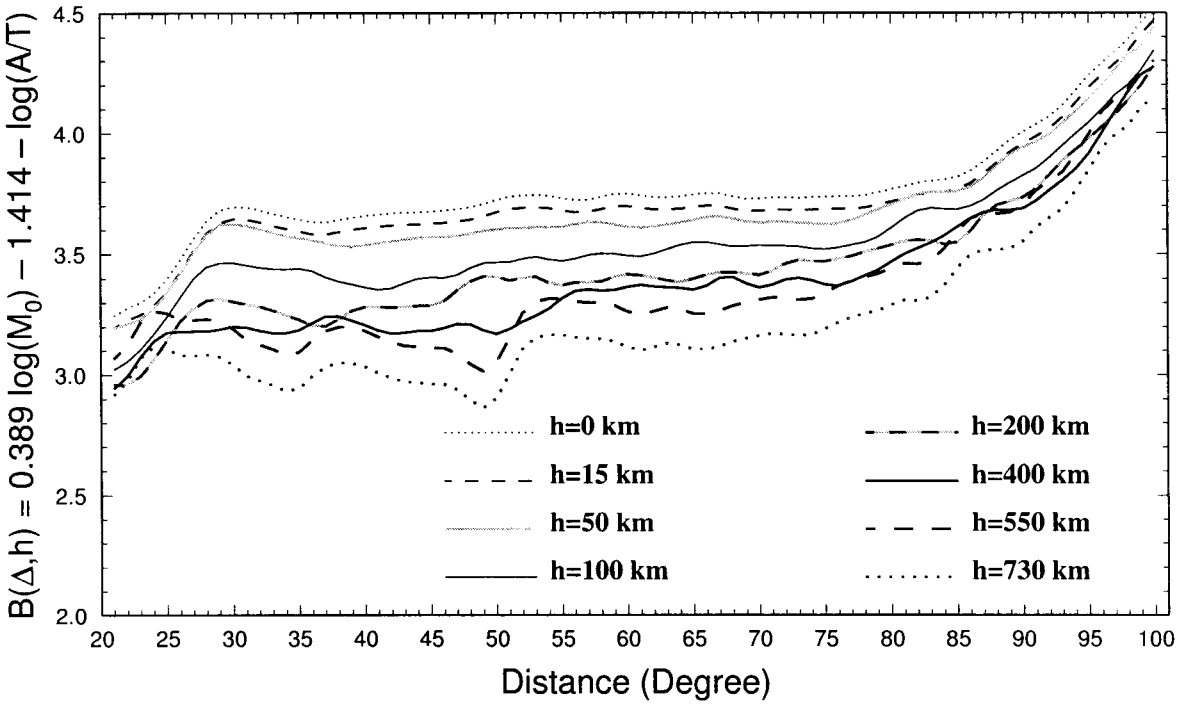

Figure 2. New depth-distance correction curves $B(\Delta,h)$ using equation (7) and M_0 values from CMT catalog. The depth-distance correction curve for zero depth was derived by adding 0.05 to depth-distance correction curve at 15 km, and the depth distance correction curve at 730 km depth was derived by subtracting 0.15 from depth-distance correction curve at 550 km.

in comparison with using the ratio of $\frac{\log(A/T)}{\log M_0}$. Also, to eliminate possible biases introduced by the saturation effect of the magnitude scale and the effect of sensitive stations on determined magnitude from small events, the procedure of obtaining $B(\Delta,h)$ curves using equation (7) was repeated excluding earthquakes with seismic moment $M_0 < 5.8 \times 10^{16}$ and $M_0 > 1.0 \times 10^{20}$ N m from dataset (see Fig. 1). The $B(\Delta,h)$ curves obtained did not change. An advantage of using log M_0 to normalize is that it forms a consistent basis for comparing events at different depths.

It is then appropriate to calibrate the scale so that the sum-squared correction needed for all ISC event magnitudes so far determined is minimized, that is, to minimize $\Sigma[m_b^{G-R} - (\overline{m_b^{New}} + \delta)]^2$ (m_b^{New} is calculated using the new correction terms obtained in this study) where the sum is over all 110,720 events between 1978 and 1993. $\delta = -0.037$ was found. The numerical values of $B(\Delta,h)$ including the value of $\delta = 0.037$ are tabulated in Table 2. The value of δ ensures there is no net offset between m_b^{G-R} and m_b^{New}.

Comparison of Different Correction Terms

In this section, the new depth-distance correction terms are compared with the Gutenberg–Richter terms, and then they are compared with other published depth-distance correction terms and applied to the ISC dataset.

In Figure 3 the Gutenberg-Richter and the new correction terms are separately compared at specific depths. Figure 3 shows that the Gutenberg–Richter correction terms for shallow depths are smaller than the new correction terms in the distance range 20°–35°, whereas in the range 45°–90° they are larger. These discrepancies are reversed at greater depths. As Figure 3 shows, the difference between estimated m_b^{G-R} and m_b^{New} depends on the distribution of observations by epicentral distance. The distributions of magnitudes for m_b^{G-R} and m_b^{New} are shown in Figure 4. To show the difference between m_b^{G-R} and m_b^{New}, the averaged $m_b^{G-R} - m_b^{New}$ values are plotted against m_b^{G-R} values in Figure 5, with the standard deviations for 60,544 out of 110,225 earthquakes and for 180 out of 420 nuclear explosions. Each point in Figure 5 represents the average $m_b^{G-R} - m_b^{New}$ values of events with the same m_b^{G-R} value and different m_b^{New} values. Figures 4 and 5 show that applying the new correction terms tends to increase small magnitudes and decrease large magnitudes, in comparison with applying the Gutenberg–Richter terms. As observed in Figure 3, the Gutenberg–Richter depth-distance correction terms in the distance range 45°–90° are greater for shallow depths than those of the new depth-distance correction terms. In the dataset the majority of events have a shallow depth, and the concentration of observations is high at this distance range. Also, most of the

Table 2
Global Depth-Distance Correction $B(\Delta,h)$ for Determination of Body-Wave Magnitude

h → / Δ ↓	15	50	100	200	400	550
21	3.233	3.232	3.059	2.995	2.980	3.104
22	3.266	3.251	3.092	2.998	3.032	3.160
23	3.289	3.268	3.143	3.032	3.110	3.256
24	3.324	3.313	3.206	3.099	3.177	3.304
25	3.383	3.379	3.279	3.180	3.213	3.295
26	3.463	3.456	3.361	3.260	3.218	3.267
27	3.549	3.542	3.436	3.314	3.219	3.266
28	3.623	3.618	3.484	3.347	3.219	3.271
29	3.668	3.659	3.500	3.353	3.227	3.260
30	3.683	3.663	3.501	3.343	3.238	3.229
31	3.681	3.655	3.491	3.332	3.235	3.183
32	3.671	3.641	3.482	3.323	3.222	3.164
33	3.655	3.626	3.476	3.307	3.212	3.144
34	3.642	3.613	3.475	3.287	3.212	3.120
35	3.631	3.604	3.477	3.267	3.224	3.132
36	3.621	3.595	3.467	3.244	3.254	3.182
37	3.619	3.583	3.443	3.240	3.282	3.220
38	3.629	3.571	3.425	3.271	3.282	3.237
39	3.639	3.568	3.414	3.305	3.264	3.236
40	3.645	3.575	3.401	3.321	3.245	3.221
41	3.651	3.583	3.391	3.321	3.223	3.196
42	3.656	3.590	3.397	3.319	3.209	3.173
43	3.659	3.598	3.417	3.321	3.214	3.158
44	3.661	3.604	3.435	3.324	3.220	3.155
45	3.664	3.608	3.441	3.326	3.220	3.150
46	3.668	3.609	3.440	3.344	3.233	3.148
47	3.673	3.612	3.451	3.388	3.250	3.126
48	3.680	3.622	3.478	3.424	3.248	3.081
49	3.694	3.633	3.499	3.446	3.223	3.051
50	3.711	3.640	3.502	3.445	3.208	3.090
51	3.723	3.644	3.504	3.428	3.229	3.193
52	3.729	3.647	3.518	3.440	3.259	3.296
53	3.731	3.648	3.526	3.444	3.284	3.343
54	3.727	3.648	3.515	3.419	3.314	3.355
55	3.718	3.651	3.508	3.409	3.357	3.354
56	3.710	3.660	3.518	3.420	3.385	3.342
57	3.712	3.671	3.533	3.421	3.393	3.338
58	3.723	3.669	3.540	3.424	3.387	3.337
59	3.734	3.659	3.539	3.444	3.390	3.326
60	3.736	3.651	3.530	3.453	3.402	3.301
61	3.728	3.647	3.527	3.449	3.410	3.288
62	3.722	3.651	3.538	3.440	3.404	3.302
63	3.722	3.659	3.556	3.428	3.401	3.318
64	3.725	3.667	3.574	3.422	3.398	3.310
65	3.731	3.679	3.585	3.435	3.391	3.293
66	3.737	3.690	3.586	3.452	3.407	3.291
67	3.737	3.693	3.577	3.460	3.438	3.305
68	3.725	3.684	3.567	3.462	3.442	3.324
69	3.715	3.672	3.569	3.456	3.416	3.339
70	3.716	3.668	3.573	3.451	3.400	3.350
71	3.720	3.670	3.571	3.467	3.410	3.359
72	3.720	3.671	3.571	3.497	3.432	3.357
73	3.719	3.668	3.568	3.512	3.438	3.349
74	3.720	3.663	3.559	3.508	3.429	3.353
75	3.723	3.661	3.556	3.506	3.412	3.378
76	3.725	3.665	3.564	3.516	3.406	3.407
77	3.725	3.679	3.575	3.529	3.425	3.427
78	3.729	3.700	3.585	3.545	3.448	3.442
79	3.741	3.721	3.608	3.559	3.470	3.455
80	3.753	3.742	3.645	3.574	3.505	3.479

Table 2 (Continued)

81	3.766	3.763	3.685	3.590	3.537	3.498
82	3.780	3.783	3.716	3.595	3.561	3.495
83	3.788	3.792	3.727	3.591	3.583	3.509
84	3.792	3.792	3.723	3.577	3.614	3.559
85	3.803	3.796	3.722	3.585	3.649	3.630
86	3.828	3.814	3.735	3.633	3.685	3.684
87	3.866	3.850	3.760	3.700	3.709	3.704
88	3.914	3.903	3.799	3.740	3.720	3.703
89	3.958	3.948	3.832	3.755	3.719	3.709
90	3.993	3.978	3.860	3.772	3.726	3.741
91	4.023	3.999	3.890	3.806	3.758	3.800
92	4.057	4.032	3.935	3.863	3.801	3.838
93	4.103	4.080	3.986	3.923	3.841	3.875
94	4.163	4.128	4.034	3.967	3.887	3.949
95	4.226	4.178	4.081	4.012	3.951	4.032
96	4.277	4.234	4.136	4.063	4.038	4.126
97	4.325	4.296	4.195	4.112	4.126	4.179
98	4.375	4.362	4.235	4.173	4.207	4.216
99	4.445	4.394	4.296	4.233	4.277	4.292
100	4.506	4.482	4.380	4.317	4.312	4.337

Δ is epicentral distance in degrees and h is focal depth in kilometers.

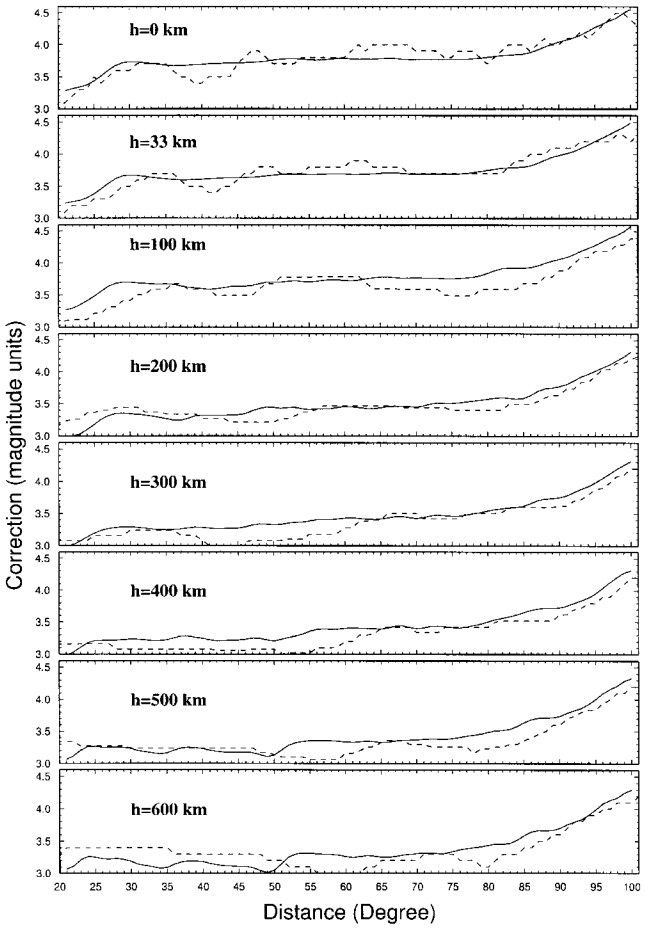

Figure 3. Comparison of depth-distance correction terms of Gutenberg and Richter (1956) with the new correction terms. In each graph the solid and the dashed lines represent the new and the Gutenberg-Richter correction curves, respectively.

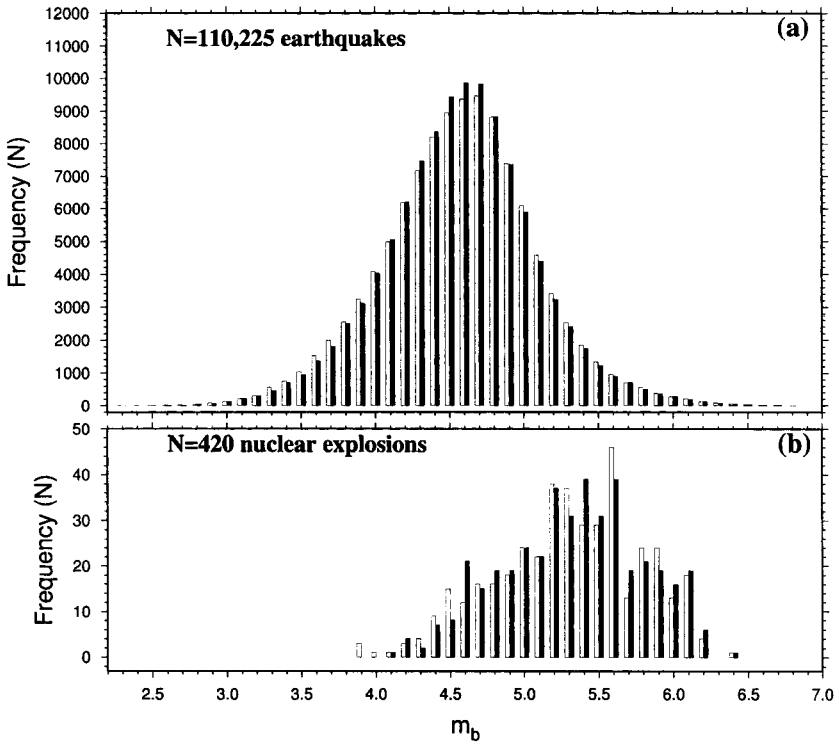

Figure 4. Distribution of m_b for 110,225 earthquakes and 420 nuclear explosions in the ISC dataset between 1978 and 1993. (a) For earthquakes, (b) for nuclear explosions. In each case the white histogram represents the frequency of m_b^{G-R} values (using Gutenberg–Richter depth-distance correction terms), and the black histogram shows the frequency of m_b^{New} values (using depth-distance correction terms obtained in this study).

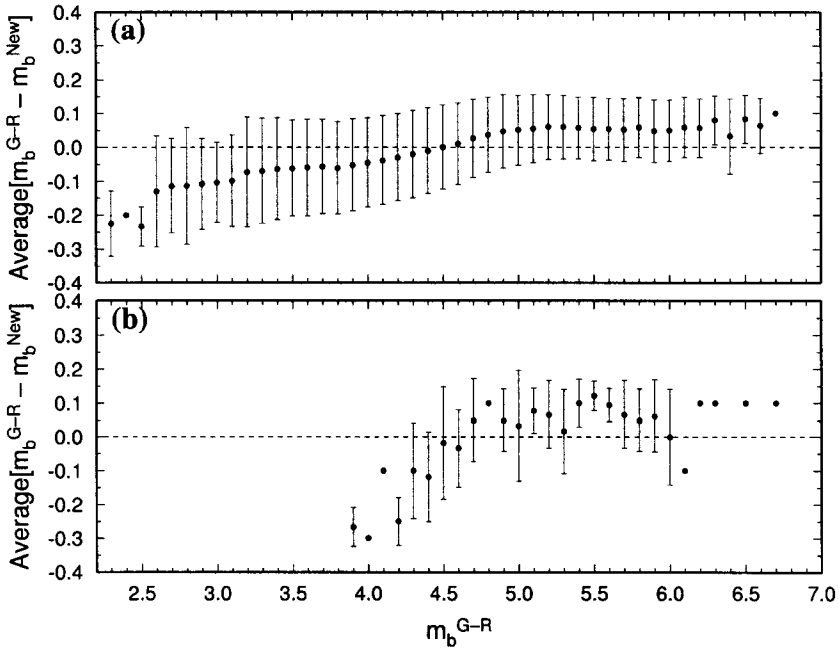

Figure 5. Average values of $m_b^{G-R} - m_b^{New}$ against m_b^{G-R} for earthquakes and explosions in which calculated m_b^{G-R} and m_b^{New} values are different. (a) For 60,544 out of 110,225 earthquakes; (b) for 180 out of 420 nuclear explosions. In each case the standard deviation of data points have been shown.

large events occurred at shallow depths and are observed at greater distances (45°–90°). Events with small sizes are generally observed at closer distances where the Gutenberg–Richter correction terms are less than those of the new correction terms. Therefore, for a dataset in seismicity studies, the *b*-value based on m_b^{New} values will be systematically higher than that for m_b^{G-R} values.

Figure 6 shows a comparison of different depth-distance correction terms versus distance. As Figure 6a shows, the variation of Gutenberg–Richter terms with distance and depth is complicated and not smooth. Nortmann and Duda (1982) stated that the strong variation with distance, which the Gutenberg–Richter correction function displayed, is simply due to scatter of the underlying observations made prior to 1955 which they used for the determination of their correction terms.

In contrast to the Gutenberg–Richter depth-distance correction curves, the curves produced by Veith and Clawson

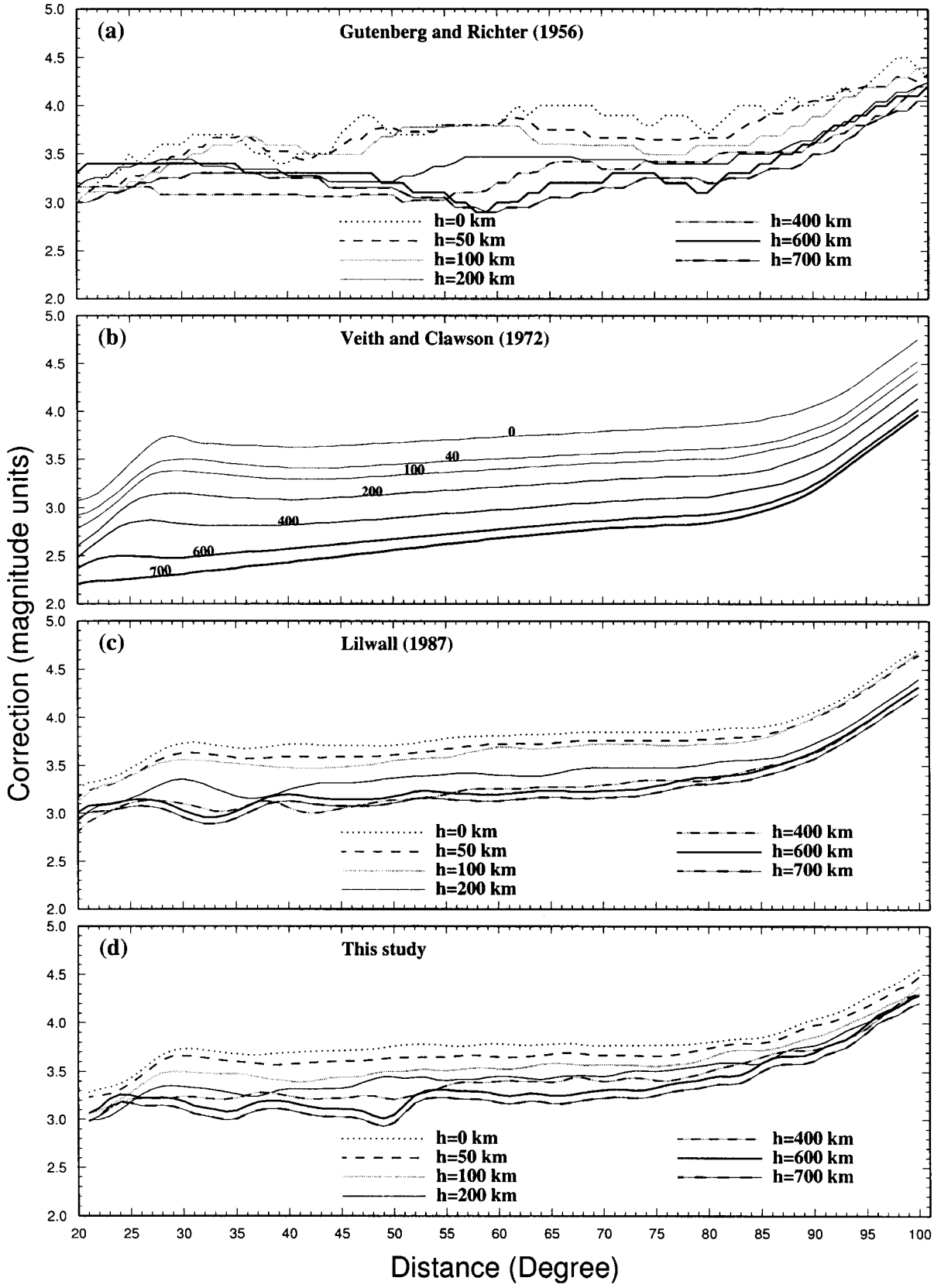

Figure 6. A comparison of different depth-distance correction curves $B(\Delta,h)$ against distance. (a) Gutenberg and Richter (1956); (b) Veith and Clawson (1972), line thickness increases with depth as annotated; (c) Lilwall (1987b); (d) this study.

(1972) (see Fig. 6b) are very smooth. Veith and Clawson obtained an empirical surface focus amplitude-distance curve using normalized log(A/T) of 43 large explosions. They used Gutenberg's (1945b) formulation and evaluated the relative amplitudes of ground displacements as the geometric spreading curve for the Herrin (1968) earth model. They then corrected the amplitudes of geometric spreading curves for attenuation corresponding to $\bar{Q}$ structure. Veith and Clawson combined the deep theoretical curves with the empirical surface curve and gave a corresponding set of depth-distance terms. Because of differences in attenuation used, they expected their correction terms to give a smaller m_b for deep earthquakes compared to the Gutenberg–Richter terms.

Ringdal (1976) found that maximum-likelihood was potentially the best technique to yield a significant improvement in network magnitude estimations of small- and medium-size events, compared to the conventional method of averaging the magnitudes of all detecting stations. Lilwall (1987b), by using a joint maximum-likelihood estimation technique and considering the station recording thresholds, determined the correction terms for m_b plotted in Figure 6c. He computed station terms only, using the shallow focus data, which were applied to all input data (including deeper focus earthquakes) in the determination of distance terms. Lilwall (1987b) normalized the baseline of his correction curves with those of Gutenberg and Richter (1956) at a distance range of 30°–90°.

Most of the correction curves in Figure 6 show considerable similarity over the distance range 30°–90°, within which the correction varies little. As Figure 6 shows, the correction curves obtained in this study, Veith-Clawson correction curves and Lilwall's curves are similar with increasing distance and depth. However, the deeper curves of Lilwall, and those of this study, are different from the Gutenberg–Richter curves. The general shape of the new depth-distance curves is similar to that of Lilwall's curves. Comparison of Figure 6c with 6d shows that the difference between depth-distance curves at 100 km and 200 km in the case of Lilwall are approximately twice that of the new depth-distance curves. Lilwall calibrated his correction curves at specific depths with those of Gutenberg and Richter; hence, observing the same discrepancy in estimated m_b^{G-R} and m_b^{L} values with depth is expected. In Figures 6c and d, $B(\Delta,h)$ curves for deeper earthquakes show more structure and irregularities.

In general, any empirical $B(\Delta,h)$ curve based on observations is obtained in practice using data over a finite depth range. Therefore, nonuniformity in distribution of events with depth, and any error in determined depths, can affect the uniformity of $B(\Delta,h)$ curves. It is well known that heterogeneity within the Earth, and in some cases, the acceptable solution of the standard least-squares analysis of location determination, affect the accuracy of the determination of earthquake locations, especially that in focal depth (Adams *et al.*, 1982; Adams, 1992). Figure 6 shows that in the cases of Gutenberg and Richter (1956), Veith-Clawson (1972), Lilwall (1987b), and this study, the difference between the average corrections over distances 20°–100° for zero and 700-km focus events are 0.56, 1.06, 0.58, and 0.52 magnitude units, respectively. In addition to the differences in the methods and observations, the main reasons for the previous discrepancy are the differences in attenuation factors and the Earth model that were used by different authors.

The ISC has extracted depth-distance correction values from Gutenberg and Richter's chart (Gutenberg and Richter, 1956) for different depths, and in determination of m_b uses the correction terms for the closest depth to the calculated depth. In this study the ISC extracted values are used with interpolation for determination of m_b^{G-R}, giving good agreement with the ISC-calculated values. Also, for the determination of m_b^{L}, m_b^{V-C}, and m_b^{New} values, the depth-distance terms are used with interpolation. The correction terms considered above were applied to 16 years of data in the ISC Bulletin between 1978 and 1993. The residual of station magnitude from event magnitude after averaging in 1-degree-wide intervals is plotted against distance in Figure 7. As this Figure shows, in all four cases the variation of δm_b is small in the distance range 30°–85°, but it is high for regional distances and distances of $\Delta > 90°$. The value of δm_b in the case of Gutenberg and Richter (1956), which is presently used by ISC and NEIC, has more variation than the others with epicentral distance. Comparison of curves in Figure 7 shows that bias in the cases of Veith and Clawson (1972), Lilwall (1987b), and this study are less than in Gutenberg and Richter (1956), but in the cases of Veith and Clawson and Lilwall, there is a systematic bias for distances beyond about 88°. Application of the new correction terms results in estimated m_b^{New} values that are independent of epicentral distance and are hence a better description of the seismic source. Note that this result was not assumed or used as a constraint. It is a positive test of the hypothesis that calibration of m_b by the M_0 scale leads to a better description of the seismic source by m_b.

To compare the estimated m_b^{G-R}, m_b^{V-C}, m_b^{L}, and m_b^{New} values using Gutenberg–Richter, Veith–Clawson, Lilwall, and new depth-distance correction terms, respectively, the estimated m_b values for 110,720 events are averaged within 20-km intervals and are plotted in Figure 8a. This figure shows that the mean m_b^{V-C} value is smaller than the others and as is expected from Figure 6b, this discrepancy increases with depth. However, the differences among the mean m_b^{G-R}, m_b^{L}, and m_b^{New} are not significant in some depth ranges, but at most depth ranges their difference are systematic and significant; for example, in the depth range of 200–550 km, the m_b^{New} is greater than m_b^{G-R} and m_b^{L}, and for $h < 200$ km, the reverse is true. Figure 8a shows that the mean m_b over 20-km intervals decreases at intermediate depths; however, we expected an increase with depth, because most of the small earthquakes at deeper depths are not recorded by seismic stations because of higher attenuation in the upper mantle. Average logM_0 and m_b^{New} values over 20-km

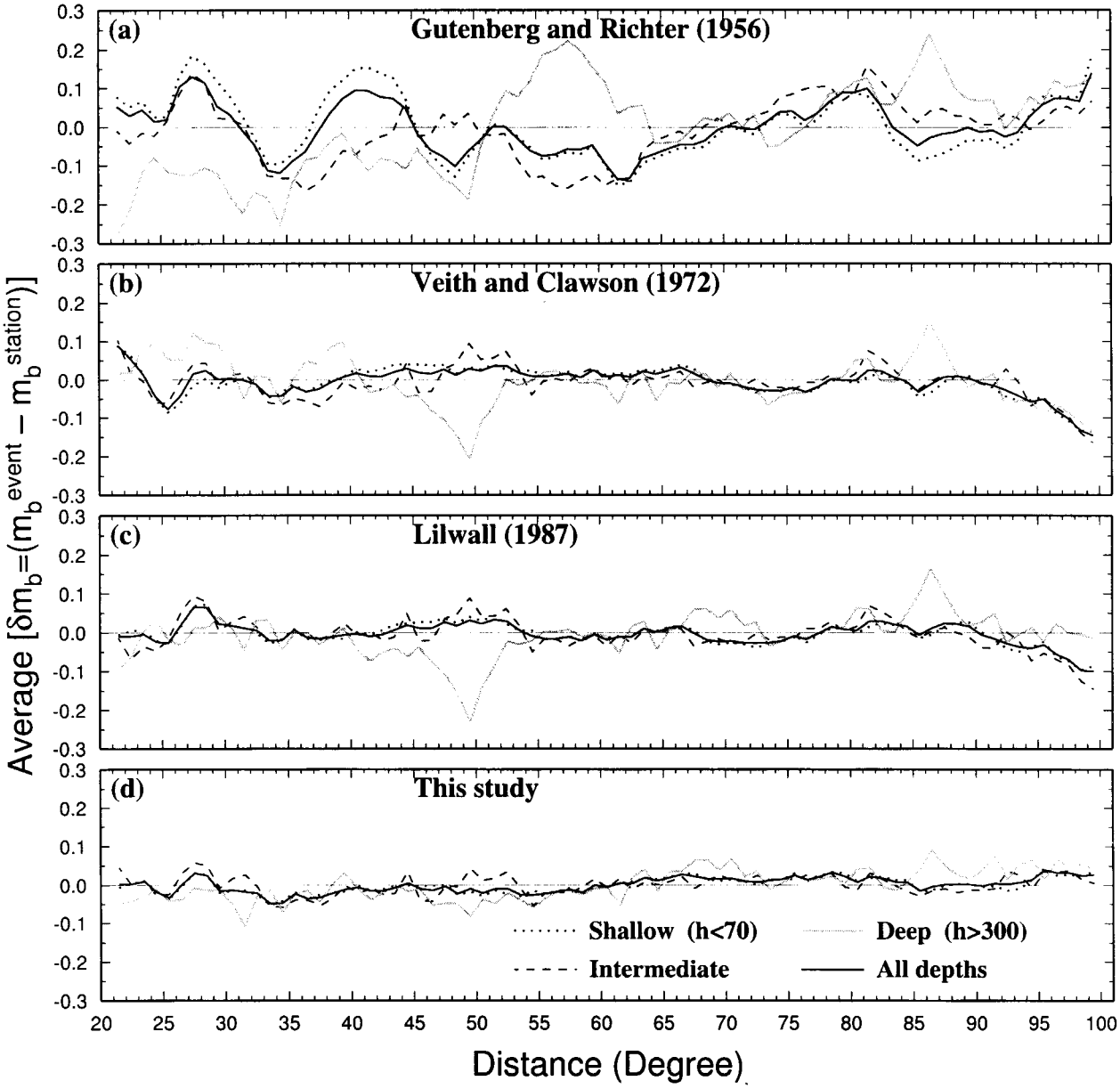

Figure 7. Comparison of averaged residual of station-magnitude from event-magnitude (mean magnitude) over 1-degree-wide intervals against distance using Gutenberg–Richter (1956), Veith–Clawson (1972), Lilwall (1987b), and new correction terms. In each case the dotted line indicates 905,785 observations from 60,631 shallow events ($h < 70$ km), the dashed line indicates 269,269 observations from 20,095 intermediate earthquakes (70 km $\leq h \leq$ 300 km), the gray-line indicates 94,141 observations from 6222 deep earthquakes (300 km $\leq h$), and the thick solid-line represents 1,269,195 observations from 86,948 events (all depths). The residual calculation excludes 23,772 events with only one observation.

depth intervals are plotted versus depth in Figure 8b and c, respectively. As Figure 8a shows, because of several factors such as stress drop and rheology, we expect to observe a variation in the average m_b or log M_0 with depth. Figure 8c shows that averaged m_b^{New} values over 20-km depth interval are approximately the same because the Harvard group selects earthquakes in a limited range of magnitude (i.e. $5 \lesssim m_b \lesssim 6$) to make the M_0 determination.

Finally estimated m_b values using four different correction terms are compared with the scalar seismic moment. Figure 9 shows a comparison of four different determinations of m_b versus log M_0 for the ISC dataset of magnitudes and depths, and the CMT catalog of seismic moment, with m_b averaged in 0.1-wide intervals in log M_0. In Figure 9, each data point on the graph indicates the position of magnitude values for earthquakes with the same log M_0 but with

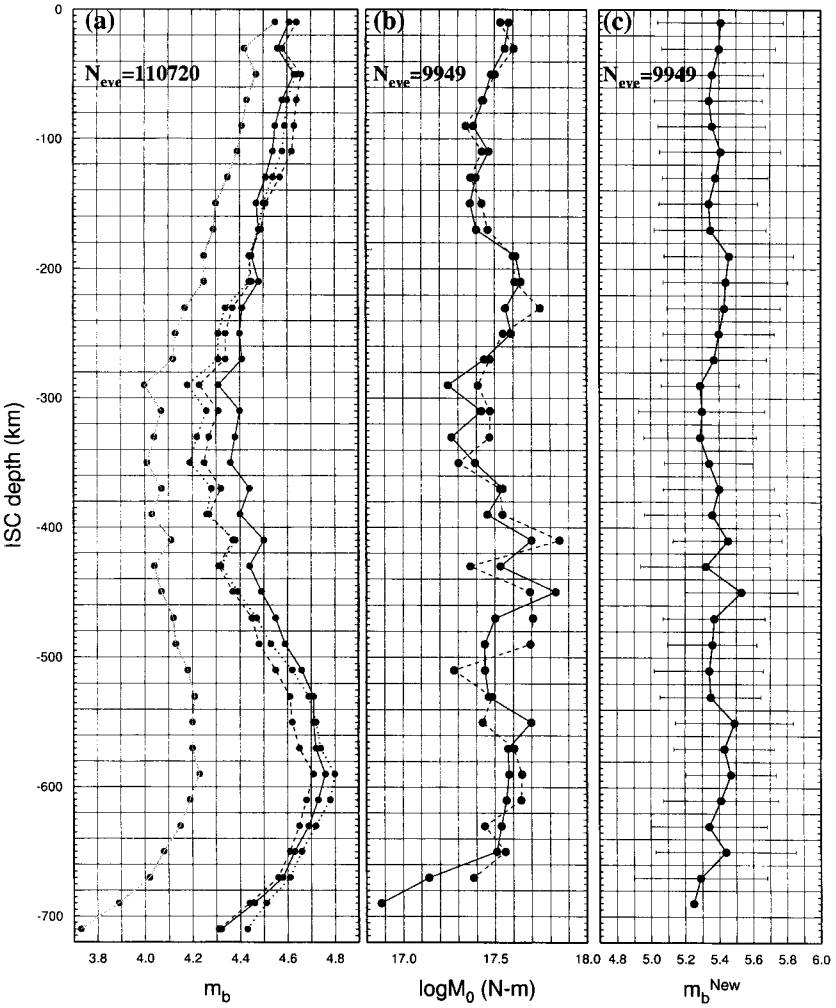

Figure 8. (a) Comparison of the mean values of magnitude distribution as a function of depth over 20-km depth intervals for 110,720 events in the dataset. Dotted, gray, dashed, and solid curves represent mean values of m_b^{G-R}, m_b^{V-C}, m_b^{L}, and m_b^{New}, respectively. (b) For each 20-km depth interval, the mean value of log M_0 for 9949 earthquakes from the Harvard CMT Catalog is shown. The events are those for which the ISC prime location information is almost identical with that in the CMT catalog. The solid and dashed lines use the ISC and CMT depths, respectively. (c) Averaged m_b^{New} values with standard deviations as a function of depth over 20-km depth intervals for 9949 earthquakes (using ISC depth).

different magnitude when averaged. As Figure 9 shows, in the cases of the Gutenberg–Richter, Veith–Clawson, and Lilwall schemes, estimated m_b values for deep earthquakes are underestimated by about 0.1–0.15, 0.3–0.5, and 0.1–0.2 magnitude units respectively compared to M_0. Application of the new depth-distance correction terms for the determination of m_b gives little bias against M_0 with depth using ISC depths, again consistent with the hypothesis that a moment-based calibration gives a better basis for m_b as a source property. Therefore, when the Gutenberg–Richter, Veith–Clawson, and Lilwall correction terms are used, the estimated m_b values show a depth dependency relative to M_0 and the m_b of deep earthquakes are systematically underestimated. This discrepancy (Fig. 9) between estimated magnitudes of earthquakes with different depths is even greater if the CMT focal depth is used instead of ISC focal depth.

Applying Station Corrections in the Determination of m_b

The station correction term mainly includes any effects due to the recording instrument and local geology around the recording station. The lithology beneath the seismic station can have an important role in attenuating or enhancing seismic arrivals (Abercrombie *et al.*, 1993). Many studies show that the station correction can be significant (e.g., Marshall *et al.*, 1979; Vila *et al.*, 1996). Correcting estimated m_b for station effects reduces the variance of the observations and so improves the precision of the estimates. Therefore, m_b estimated using station corrections should give the best relative magnitudes for the sources. To determine station corrections, a uniform spatial distribution of events is desirable. Clearly on a global scale, this is impractical. Here the station correction was calculated empirically for each station by averaging residuals from event magnitude (events in which more than two stations contributed to the determination of $\overline{m_b}$). For each station, four different sets of station terms were calculated using magnitudes that were estimated using four different depth-distance correction terms. The correction values for those 267 seismic stations at which the ISC has more than 1000 measurement from 1978 to 1993 are tabulated in Table 3. The resulting station corrections were then used for determining event magnitude, but only at 458 stations for which the ISC used more than 200 observations in calculating event magnitude between 1978 to

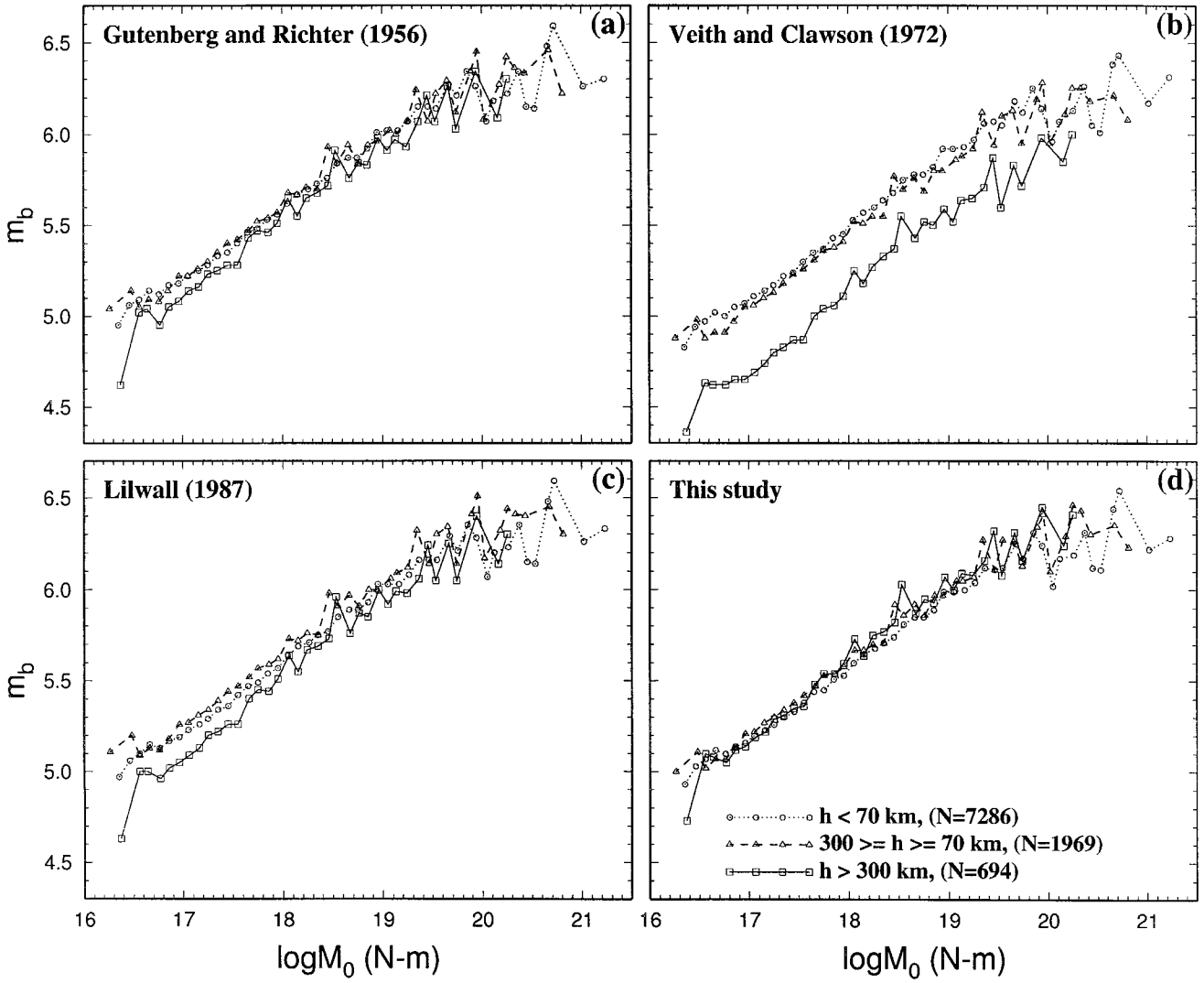

Figure 9. Averaged m_b values in 0.1-wide intervals of log M_0 versus log M_0 using four different depth-distance correction terms. (a) Gutenberg-Richter, (b) Veith-Clawson, (c) Lilwall, (d) the new depth-distance correction terms. Note, the data were grouped (shallow, intermediate, and deep) according to ISC depth.

1993. For other stations, for which ISC has used 200 or fewer observations, magnitudes were calculated without using station corrections. The resulting residuals after applying station corrections are shown as a function of epicentral distance in Figure 10.

As Figure 10 shows, using station corrections generally reduces the residuals in comparison with Figure 7, which shows magnitudes calculated without station corrections. In the distance range of 40°–80°, residuals that are originally small (without using station correction) do not change much. The negative peak at distance about $\Delta = 50°$ for deep earthquakes disappears, but the positive peak of residuals at distance about 87° for deep earthquakes does not. This shows the effect of station residual combined with nonrandom source/distance distribution for deep earthquakes.

Using station corrections, the residuals at all depths are significantly increased in the negative direction at distances greater than ~80° but are slightly increased in the positive direction at distances less than ~80° (compare Fig. 10 with Fig. 7). This systematic result does not change when applying station corrections to the whole dataset without restriction. The station correction terms that were used in Figure 10 were averaged over 1-degree-wide intervals of epicentral distance for each set of correction terms separately. In all four cases the averaged station corrections are approximately independent of distance up to about 88°, but for $\Delta > 88°$, they progressively increase. At $\Delta > 88°$, due to the core shadow zone, the amplitude of observations quickly decays with distance. The main reasons for the apparent increase in the negative direction are the nonrandom distribution of

Table 3
Mean Deviation $\overline{\delta m_b}$ of all values of $\delta m_b = \overline{m_b} - m_b^{Station*}$ for Those 267 Seismic Stations at Which the ISC Has Used More Than 1000 Measurements between 1978 and 1993

1	2	3
ABU	−0.23 ± 0.33	1564
ADE	−0.40 ± 0.32	4720
ADK	−0.20 ± 0.37	1502
AFR	−0.05 ± 0.29	2337
AKU	−0.24 ± 0.50	2538
ALE	0.18 ± 0.29	6142
ALQ	0.26 ± 0.28	16180
ANMO	0.17 ± 0.34	1388
ANR	−0.44 ± 0.27	1397
ARMA	0.11 ± 0.27	2112
ARU	−0.38 ± 0.26	1489
ASP	−0.25 ± 0.31	1270
ASPA	−0.13 ± 0.35	15664
AVF	0.09 ± 0.23	11351
BAG	−0.23 ± 0.35	1162
BAL	0.00 ± 0.29	1428
BCAO	−0.08 ± 0.35	3421
BDT	−0.06 ± 0.36	4907
BDW	0.25 ± 0.32	6526
BFD	−0.01 ± 0.29	1298
BGF	0.06 ± 0.23	4394
BHG	−0.15 ± 0.23	1110
BHO	0.13 ± 0.37	1658
BJI	0.00 ± 0.34	6376
BKR	−0.30 ± 0.29	1151
BKS	−0.23 ± 0.57	3853
BLA	−0.07 ± 0.34	1945
BMN	0.23 ± 0.33	4799
BNG	−0.13 ± 0.30	8585
BOD	0.04 ± 0.31	2591
BRG	0.05 ± 0.22	9536
BRS	0.38 ± 0.39	1948
BSF	0.13 ± 0.23	6477
BUL	0.12 ± 0.29	8431
BW06	0.21 ± 0.30	5763
CAF	0.08 ± 0.23	6496
CD2	−0.26 ± 0.28	1909
CDF	0.19 ± 0.24	6359
CHG	0.09 ± 0.30	9431
CHTO	0.23 ± 0.34	8390
CIR	0.31 ± 0.27	1418
CLK	0.30 ± 0.28	1507
CLL	−0.08 ± 0.22	8985
CMB	0.19 ± 0.32	1042
CMS	0.07 ± 0.32	1913
CN2	0.14 ± 0.43	2721
CNB	−0.07 ± 0.29	1510
COL	−0.05 ± 0.30	7626
COO	−0.13 ± 0.34	1046
COP	−0.29 ± 0.24	1832
CTA	−0.01 ± 0.33	9768
CTAO	0.03 ± 0.31	3606
CVF	0.08 ± 0.28	1716
CYP	−0.98 ± 0.45	2793
DAG	0.00 ± 0.30	10274
DCN	−0.32 ± 0.24	1419
DIX	−0.11 ± 0.39	4261
DLE	−0.25 ± 0.26	1521
DMN	−0.27 ± 0.26	8202

(*continued*)

Table 3
Continued

1	2	3
DMU	−0.27 ± 0.25	1732
DOU	−0.13 ± 0.29	1271
DUG	0.21 ± 0.32	2240
EAB	−0.04 ± 0.29	1078
EBH	−0.09 ± 0.27	1112
ECP	−0.37 ± 0.26	1345
EDM	−0.40 ± 0.25	2499
EKA	0.10 ± 0.28	9785
ELT	−0.11 ± 0.31	2153
EMS	−0.31 ± 0.27	1531
ENN	−0.03 ± 0.27	4356
EPF	0.14 ± 0.28	4659
ESK	−0.11 ± 0.27	1020
EUR	0.15 ± 0.54	10700
FBA	0.05 ± 0.36	9623
FFC	−0.02 ± 0.29	11903
FLN	−0.01 ± 0.24	6700
FORR	−0.31 ± 0.30	1701
FRB	−0.14 ± 0.32	1652
FRF	0.03 ± 0.22	3272
FRU	−0.24 ± 0.30	1421
FUR	−0.27 ± 0.28	1743
FVM	−0.15 ± 0.32	3457
GBA	0.22 ± 0.33	19055
GDH	0.05 ± 0.30	1724
GEC2	0.50 ± 0.28	4269
GKN	−0.32 ± 0.27	3812
GLD	−0.18 ± 0.29	2780
GOL	0.15 ± 0.35	6588
GRF	−0.14 ± 0.25	6907
GRR	−0.05 ± 0.23	7532
GTA	0.05 ± 0.37	5885
GUA	−0.36 ± 0.32	2709
GUMO	−0.40 ± 0.37	1423
GUN	−0.43 ± 0.26	3991
GYA	−0.01 ± 0.36	2182
HAU	0.15 ± 0.23	6651
HFS	0.03 ± 0.33	25239
HHC	−0.03 ± 0.33	2561
HOF	−0.05 ± 0.25	1146
HYB	−0.18 ± 0.27	6710
ILT	−0.05 ± 0.29	1700
IMA	0.21 ± 0.31	6700
INK	−0.02 ± 0.36	4885
IPM	−0.06 ± 0.30	5628
IRK	0.09 ± 0.29	1744
JCT	0.06 ± 0.30	4500
JOS	−0.01 ± 0.32	1633
KAF	0.05 ± 0.28	3206
KBA	−0.03 ± 0.30	5874
KEV	0.01 ± 0.37	4693
KGM	−0.19 ± 0.37	1273
KHC	0.14 ± 0.26	5976
KIC	−0.24 ± 0.31	2880
KIR	−0.53 ± 0.24	3200
KJF	−0.13 ± 0.32	9172
KKM	−0.09 ± 0.36	1512
KKN	−0.24 ± 0.27	10480
KLB	0.00 ± 0.30	2197
KMI	−0.17 ± 0.52	3217
KNA	−0.21 ± 0.28	1496

(*continued*)

Table 3
Continued

1	2	3
KRA	−0.28 ± 0.25	4861
KRI	0.21 ± 0.28	4432
KSP	−0.01 ± 0.50	2509
LBF	0.19 ± 0.23	9040
LDF	0.02 ± 0.22	4936
LEM	−0.05 ± 0.35	1894
LFF	−0.06 ± 0.22	7322
LIC	−0.08 ± 0.28	1285
LLS	−0.30 ± 0.31	2744
LMR	0.03 ± 0.25	3989
LOR	0.12 ± 0.24	11505
LPB	−0.24 ± 0.32	2360
LPF	−0.01 ± 0.23	6761
LPG	0.04 ± 0.23	6168
LPL	0.05 ± 0.25	3199
LPO	0.04 ± 0.24	6350
LRG	−0.04 ± 0.24	3943
LSA	0.10 ± 0.40	1024
LSF	0.03 ± 0.24	6857
LTX	0.26 ± 0.33	1349
LZH	−0.18 ± 0.40	9293
MAF	0.02 ± 0.24	5506
MAIO	0.28 ± 0.30	1144
MAT	0.08 ± 0.32	9093
MAW	0.03 ± 0.29	2039
MBC	0.03 ± 0.31	21074
MBL	−0.03 ± 0.31	3562
MDJ	−0.04 ± 0.31	1515
MEK	−0.05 ± 0.32	1413
MFF	0.02 ± 0.23	7134
MGD	−0.15 ± 0.28	1175
MMK	−0.38 ± 0.29	2315
MOX	−0.08 ± 0.22	6298
MOY	−0.08 ± 0.28	1322
MRWA	0.20 ± 0.31	2396
MSO	0.05 ± 0.37	1554
MTD	0.23 ± 0.28	3906
MTN	−0.33 ± 0.33	1236
MUD	0.07 ± 0.32	1481
MUN	−0.11 ± 0.38	1623
MZF	0.07 ± 0.25	4427
NAI	−0.07 ± 0.36	1826
NANU	−0.03 ± 0.30	1499
NAO	0.19 ± 0.28	4169
NAU	−0.03 ± 0.32	1456
NB2	0.22 ± 0.27	25788
NDI	−0.10 ± 0.48	3831
NEW	0.04 ± 0.34	4235
NIE	−0.08 ± 0.25	3735
NJ2	0.05 ± 0.36	1137
NNA	0.13 ± 0.45	1139
NRI	0.04 ± 0.29	1615
NUR	−0.05 ± 0.40	10968
NWAO	0.07 ± 0.32	2296
OBN	−0.32 ± 0.28	3206
OGA	−0.06 ± 0.23	1731
OSS	−0.26 ± 0.26	1578
OTT	−0.04 ± 0.32	1542
PAE	0.01 ± 0.29	2506
PCT	0.26 ± 0.37	1936
PEC	0.20 ± 0.34	1103

(*continued*)

Table 3
Continued

1	2	3
PKI	−0.09 ± 0.28	9537
PME	0.04 ± 0.32	1796
PMG	−0.25 ± 0.28	2351
PMO	−0.03 ± 0.32	4175
PMR	0.02 ± 0.32	8423
PNT	−0.03 ± 0.27	8712
POO	−0.10 ± 0.31	1187
PPI	−0.04 ± 0.37	1794
PPN	0.10 ± 0.30	2551
PPT	−0.10 ± 0.29	2583
PRA	−0.07 ± 0.24	2478
PRU	0.07 ± 0.24	3396
PRZ	−0.25 ± 0.29	1248
PSI	−0.04 ± 0.33	5074
QIS	0.03 ± 0.37	1333
RES	0.08 ± 0.31	4079
RJF	0.08 ± 0.23	6265
RKG	0.02 ± 0.33	1103
RMQ	−0.18 ± 0.32	1910
RSNT	−0.03 ± 0.32	1461
RSNY	0.05 ± 0.31	1689
RSON	−0.07 ± 0.30	3198
RSSD	0.07 ± 0.29	4254
RUV	−0.03 ± 0.30	4251
SAX	−0.17 ± 0.24	1493
SBA	−0.16 ± 0.42	2047
SBF	−0.14 ± 0.22	2353
SCH	−0.18 ± 0.31	1733
SCO	0.07 ± 0.40	1261
SEK	−0.06 ± 0.35	1038
SES	−0.35 ± 0.28	2623
SKO	−0.34 ± 0.38	1239
SLE	−0.21 ± 0.25	2002
SLL	−0.05 ± 0.34	2118
SLR	−0.09 ± 0.34	2069
SMF	0.04 ± 0.23	10666
SNG	0.03 ± 0.67	1239
SNY	−0.05 ± 0.34	1679
SPA	−0.01 ± 0.34	15161
SSC	0.09 ± 0.24	1754
SSE	0.15 ± 0.51	4380
SSF	0.14 ± 0.23	10868
STK	0.25 ± 0.42	6641
SUF	0.06 ± 0.28	13582
SVE	−0.26 ± 0.27	1453
SVW	−0.10 ± 0.32	1499
TBI	−0.05 ± 0.30	1132
TCF	0.15 ± 0.23	8762
TIC	−0.03 ± 0.28	1091
TIK	−0.01 ± 0.33	2483
TLG	0.15 ± 0.34	1671
TMA	−0.45 ± 0.25	2062
TNP	0.21 ± 0.29	3880
TOL	−0.06 ± 0.64	1585
TOO	−0.10 ± 0.30	3125
TPT	−0.03 ± 0.31	4189
TRT	−0.13 ± 0.35	1363
TTA	0.18 ± 0.29	2319
TUC	0.13 ± 0.32	1074
TUL	−0.10 ± 0.32	10426
TVO	−0.12 ± 0.28	2690

(*continued*)

Table 3
Continued

1	2	3
UPP	−0.47 ± 0.24	3333
UZH	−0.16 ± 0.33	1308
VAH	0.06 ± 0.31	3821
VAL	−0.21 ± 0.26	1021
VDL	−0.45 ± 0.24	1597
WARB	0.06 ± 0.31	2563
WB2	−0.09 ± 0.39	5392
WBN	−0.13 ± 0.29	1764
WET	−0.04 ± 0.24	1741
WHN	−0.01 ± 0.56	1643
WIN	−0.05 ± 0.33	1065
WMQ	0.00 ± 0.37	2774
WR2	−0.07 ± 0.39	1644
WRA	0.25 ± 0.35	31859
WTS	−0.01 ± 0.27	4343
WTTA	−0.12 ± 0.24	1087
XAN	0.07 ± 0.31	2989
YAK	−0.40 ± 0.28	2771
YKA	0.36 ± 0.33	7338
YKC	−0.02 ± 0.30	5125
YSS	−0.06 ± 0.36	1140
ZAK	0.12 ± 0.30	3629
ZLA	−0.56 ± 0.23	1022
ZOBO	0.11 ± 0.34	2958
ZUL	−0.36 ± 0.26	2840

*m_b values are determined using new depth-distance calibration terms. 1, station code; 2, station correction with standard deviation ($S_c = \overline{\delta m_b} \pm \sigma_{mean}$) using m_b^{New} values; 3, number of readings.

anomalous stations and the nonrandom source/distance distribution.

The standard deviation of the individual mean magnitudes, for events in which two or more observations have been used in calculating the mean magnitude, are compared in Figure 11 for different depth-distance correction terms. In Figure 11b, station corrections have been included, but not in Figure 11a. Figure 11b shows that inclusion of station corrections reduces the average standard deviations by about 0.07 magnitude units, which is statistically significant. Figure 11a and b shows that standard deviations of event magnitudes for the case of Gutenberg–Richter depth-distance correction terms are larger than for the other terms. The distribution of the number of single station m_b observations for 86,948 events in which ISC has used more than one station magnitude for calculating the event magnitude is shown in Figure 11c. Magnitude is a parameter that has a great azimuthal variation due to the radiation pattern and so forth, and a reliable estimated value (event magnitude) can be made only by averaging many station magnitudes with good azimuthal coverage.

Conclusions

A large and systematic bias with epicentral distance in magnitudes calculated using Gutenberg–Richter depth-distance correction terms has shown that these terms need to be revised. New empirical global depth-distance correction terms for the determination of m_b have been determined using M_0 values. Comparison of magnitude values, computed using the depth-distance correction terms of this study and major previous studies, result in several important conclusions: (1) Comparison of event magnitude m_b calculated using the Gutenberg–Richter correction terms, and that of this study, shows that the new correction terms systematically increase small magnitudes and decrease large magnitudes. Therefore, for a dataset in seismicity studies, the *b*-value based on m_b^{New} values will be systematically higher than that for m_b^{G-R} values. (2) Comparison of the Gutenberg–Richter, Veith–Clawson, and Lilwall correction terms with the correction terms obtained in this study has shown that m_b is biased most with respect to distance when using the correction terms of Gutenberg and Richter, although a systematic bias in the estimated m_b for distance greater than 88° is observed when Veith and Clawson and Lilwall's terms are used. (3) In the cases of using the correction terms of Gutenberg and Richter, Veith and Clawson, and Lilwall, the estimated m_b values for deep earthquakes are underestimated by about 0.1–0.15, 0.3–0.5, and 0.1–0.2 magnitude units, respectively, relative to m_b^{New}. (4) Application of the new correction terms to the ISC dataset has shown that estimated m_b is independent of distance and focal depth and provides unbiased estimates of m_b in comparison with other correction terms, even though this was not introduced as an a prior constraint. This implies that the new m_b values are a better measure of the size of the seismic source. (5) The standard deviations of m_b values for single events are compared in Figure 11 for each set of correction terms. This has shown that the Gutenberg–Richter standard deviations are consistently larger than those for Veith and Clawson, Lilwall, and this study. Station corrections obtained from station residuals have been applied using only stations for which ISC have used more than 200 observations in calculating event magnitudes between 1978 to 1993. The station corrections reduce the average standard deviation of event m_b values by about 0.07 magnitude units, which is statistically significant.

The kind of study reported here is important in the removal of bias in m_b. It is also important in the correct application of the M_s:m_b criterion, explosion yield estimation, and seismicity studies.

Acknowledgments

The author sincerely thanks Prof. Alan Douglas, and Drs. Robert Pearce, Ian Main, David Bowers, and Paul Burton for their valuable comments. The author also thanks associate editor Dr. Anton M. Dainty, reviewers Prof. Paul Richards, and Mr. John R. Murphy for their valuable comments and suggesting improvements to the original manuscript. Funding from the Research Council of the University of Tehran is greatly appreciated. The figures were prepared using Generic Mapping Tools (Wessel and Smith, 1995).

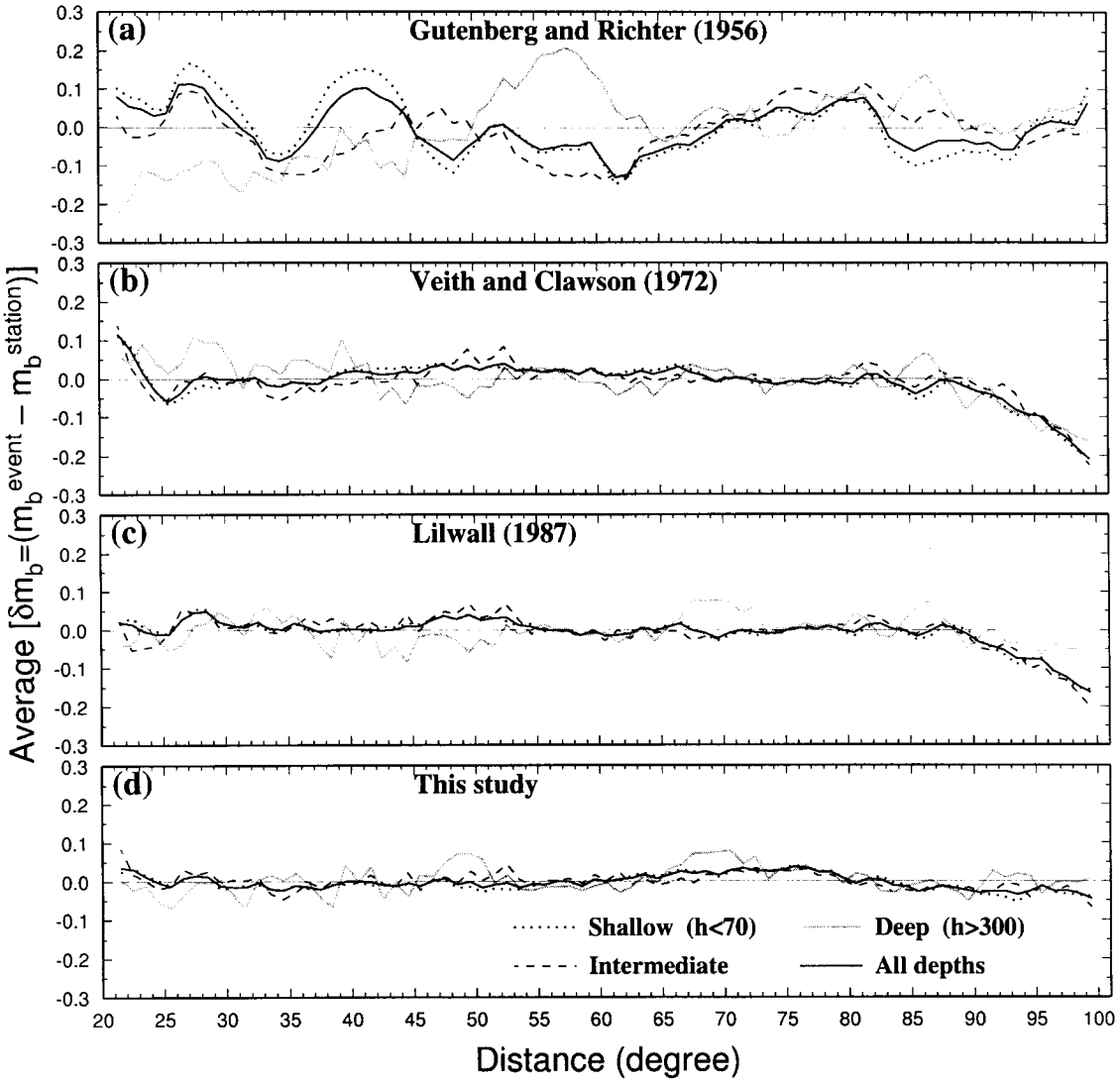

Figure 10. Comparison of average residual of station-magnitude from event-magnitude over 1-degree-wide intervals against distance, for 110,720 events using different depth-distance correction terms, and applying station corrections in the determination of m_b. (a) Gutenberg–Richter, (b) Veith-Clawson, (c) Lilwall, (d) this study.

References

Abercrombie, R. E., and P. Leary (1993). Source parameters of small earthquakes recorded at 2.5 km depth, Cajon Pass, southern California: implications for earthquake scaling, *Geophys. Res. Lett.* **20,** 1511–1514.

Adams, R. D. (1992). Effects of heterogeneity on earthquake location at ISC, *Phys. Earth Planet. Inter.* **75,** 1–5.

Adams, R. D., A. A. Hughes, and D. M. McGregor (1982). Analysis procedures at the International Seismological Center, *Phys. Earth Planet. Inter.* **30,** 85–93.

Båth, M. (1981). Earthquake magnitude—recent research and current trends, *Earth Sci. Rev.* **17,** 315–398.

Booth, D. C., P. D. Marshall, and J. B. Young (1974). Long and short period *P*-wave amplitudes from earthquakes in the range 0°–114°, *Geophys. J. R. Astr. Soc.* **39,** 523–537.

Burridge, R., and L. Knopoff (1964). Body force equivalents for seismic dislocations, *Bull. Seism. Soc. Am.* **54,** 1875–1888.

Carpenter, E. W., P. D. Marshall, and A. Douglas (1967). The amplitude-distance curve for short period teleseismic *P*-wave, *Geophys. J. R. Astr. Soc.* **13,** 61–70.

Christoskov, L., N. V. Kondorskaya, and J. Vaněk (1979). Homogeneous magnitude system of the Eurasian continent: P waves, Report SE-18, World Data Center A for Solid Earth Geophysics, Boulder, Colorado, 57 pp.

Christoskov, L., N. V. Kondorskaya, and J. Vaněk (1985). Magnitude calibrating function for a multidimensional homogeneous system of reference stations, *Tectonophysics* **118,** 213–226.

Christoskov, L., N. V. Kondorskaya, and J. Vaněk (1991). Homogeneous magnitude system with unified level for using in seismological practice, *Studies Geophys. Geod.* **35,** 221–223.

Cleary, J. (1967). Analysis of the amplitudes of short-period *P*-waves recorded by Long Range Seismic Measurements Stations in the distance range 30° to 120°, *J. Geophys. Res.* **72,** 4705–4712.

Duda, S. J. (1989). Earthquakes: magnitude, energy, and intensity, in *En-*

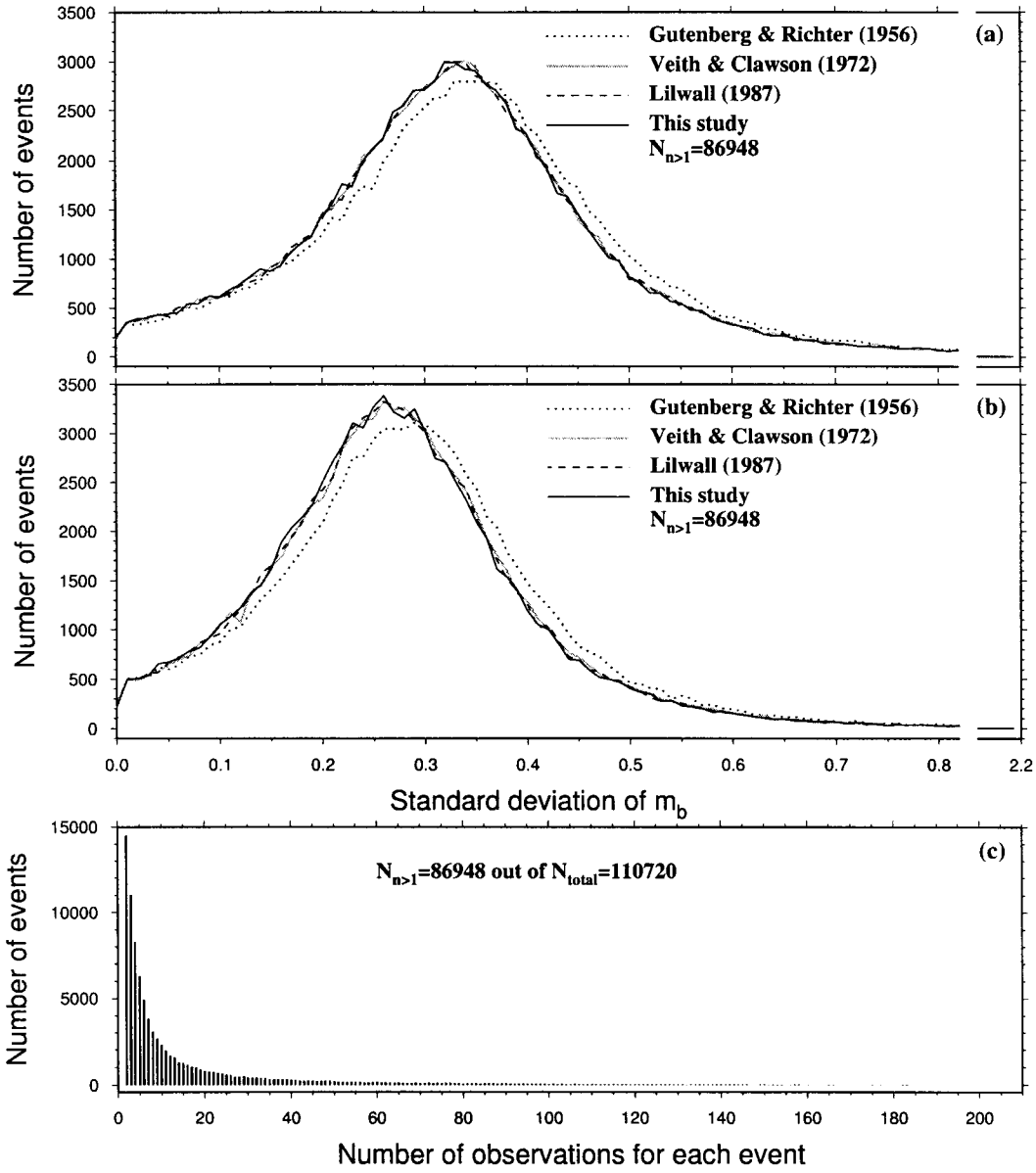

Figure 11. (a) Comparison of standard deviation of event magnitude using different depth-distance correction terms without station corrections. (b) As (a) but including station corrections. (c) Frequency of events versus number of station observations which have been used in calculating event magnitude in the ISC catalog. Events with only one observation have been excluded.

cyclopedia of Solid Earth Geophysics, D. James (Editor), Van Nostrand-Reinhold, New York, p 272–288.

Duda, S. J., T. B. Yanovskaya, E. N. Its, and R. Nortmann (1989). Preliminary reference calibrating functions for body-wave magnitudes: refracted P-waves, *Tectonophysics* **166,** 189–203.

Evernden, J. F. (1967). Magnitude determination at regional and near-regional distances in the United States, *Bull. Seism. Soc. Am.* **57,** 591–639.

Gutenberg, B. (1945a). Amplitudes of surface waves and magnitudes of shallow earthquakes, *Bull. Seism. Soc. Am.* **35,** 3–12.

Gutenberg, B. (1945b). Amplitudes of *P, PP*, and *S* and magnitude of shallow earthquakes, *Bull. Seism. Soc. Am.* **35,** 57–69.

Gutenberg, B. (1945c). Magnitude determination for deep-focus earthquakes, *Bull. Seism. Soc. Am.* **35,** 117–130.

Gutenberg, B., and C. F. Richter (1956). Magnitude and energy of earthquakes, *Ann. Geof.* **9,** 1–15.

Haskell, N. A. (1964). Total energy and energy spectral density of elastic wave radiation from propagating faults, *Bull. Seism. Soc. Am.* **56,** 1811–1842.

Herrin, E. (1968). Introduction to "1968 seismological tables for P phases," *Bull. Seism. Soc. Am.* **65,** 1073–1095.

Kanamori, H. (1983). Magnitude scale and quantification of earthquakes, *Tectonophysics* **93,** 195–199.

Kanamori, H., and D. L. Anderson (1975). Theoretical bases of some empirical relations in seismology, *Bull. Seism. Soc. Am.* **56,** 1811–1842.

Kawakatsu, H. (1995). Automated near-realtime CMT inversion, *Geophys. Res. Lett.* **22,** 2569–2572.

Lilwall, R. C. (1987a). Station threshold bias in short-period amplitude

distance and station terms used to compute body-wave magnitude m_b, *Geophys. J. R. Astr. Soc.* **91,** 1127–1133.

Lilwall, R. C. (1987b). Empirical amplitude-distance/depth curves for short-period *P* waves in the distance range 20 to 180°, AWRE Report No. O 30/86, HMSO, London.

Marshall, P. D., J. Bingham, and J. B. Young (1986). An analysis of *P*-wave amplitudes recorded by seismological stations in the USSR, *Geophys. J. R. Astr. Soc.* **84,** 71–91.

Marshall, P. D., D. L. Springer, and H. C. Rodean (1979). Magnitude correction for attenuation in the upper mantle, *Geophys. J. R. Astr. Soc.* **57,** 609–638.

Nortmann, R., and S. J. Duda (1982). The amplitude spectra of *P*- and *S*-waves and the body-wave magnitude of earthquakes, *Tectonophysics* **84,** 41–45.

Nortmann, R., and S. J. Duda (1983). Determination of spectral properties of earthquakes from their magnitudes, *Tectonophysics* **93,** 251–275.

Ringdal, F. (1976). Maximum-likelihood estimation of seismic magnitude, *Bull. Seism. Soc. Am.* **66,** 789–802.

Scheidegger, A. E. (1985). Recent research on the physical aspects of earthquakes, *Earth Sci. Rev.* **22,** 173–229.

Vaněk, J., N. V. Kondorskaya, I. V. Fedorova, and L. Christoskov (1982). Optimization of amplitude curves of seismic *P*-, *S*- and *L*-waves in the homogeneous magnitude system of the Eurasian continent, *Tectonophysics* **84,** 41–45.

Veith, K. F., and G. E. Clawson (1972). Magnitude from short-period *P*-wave data, *Bull. Seism. Soc. Am.* **62,** 435–452.

Venables, W. N., and B. D. Ripley (1999). *Modern Applied Statistic with S-PLUS*, Third Ed., Springer, New York.

Vila J., J. Batllo, and A. M. Correig (1996). Lateral variations of the local magnitude at Ebre station, Northeastern Iberian Peninsula, *Pure Appl. Geophys.* **147,** 131–146.

Wessel, P., and W. H. F. Smith (1995). New version of the Generic Mapping Tools released, *EOS* **76,** 329.

Institute of Geophysics
University of Tehran
P.O. Box 14155-6466
Tehran, Iran

Manuscript received 26 February 2002.